iSHELL: construction, assembly and testing

John Rayner*[a], Alan Tokunaga[a], Dan Jaffe[b], Morgan Bonnet[a], Greg Ching[a], Mike Connelley[a], Dan Kokubun[c], Charles Lockhart[a], Eric Warmbier[a]
[a]University of Hawaii, 2680 Woodlawn Drive, Honolulu, HI, USA 96822-0345; [b]The University of Texas Department of Astronomy, RLM 16.342, Austin, Texas, USA 78712;
[c]Oceanit, 828 Fort Street Mall Suite 600, Honolulu, Hi, USA 96813

ABSTRACT

iSHELL is 1.1-5.3 μm high spectral resolution spectrograph being built for the NASA Infrared Telescope Facility on Maunakea, Hawaii. Dispersion is accomplished with a silicon immersion grating in order to keep the instrument small enough to be mounted at the Cassegrain focus of the telescope. The white pupil spectrograph produces resolving powers of up to R=75,000 (0.375″ slit). Cross-dispersing gratings mounted in a tilt-able mechanism allow observers to select different wavelength ranges and, in combination with a slit wheel and Dekker mechanism, slit widths ranging from 0.375″ to 4.0″ and slit lengths ranging from 5″ to 25″. One Teledyne 2048x2048 Hawaii 2RG array is used in the spectrograph, and one Raytheon 512x512 Aladdin 2 array is used in a slit viewer for object acquisition and guiding. First light is expected in July 2016. In this paper we discuss details of the construction, assembly and laboratory testing.

Keywords: infrared spectrograph, cryogenic, immersion grating

1. INTRODUCTION

The NASA Infrared Telescope Facility (IRTF) is a 3-m telescope on the summit of Maunakea, Hawaii. The University of Hawaii operates the IRTF under a contract with NASA. Observing time is open to the entire astronomical community, with 50% of the observing time reserved for NASA mission support and studies of solar system objects. Available instruments include: SpeX, a 0.8-5.5 μm cross-dispersed medium-resolution spectrograph (R≤2,500) and imager; CSHELL, a 1.1-5.5 μm high-resolution spectrograph (R≤40,000); MORIS, a CCD camera mounted at the side-facing dichroic-fed window of the SpeX cryostat (MORIS can be used simultaneously with SpeX); and visitor instruments. MIRSI, a 10-20 μm camera, is currently being upgraded and will be available in 2017. Information on available instruments can be found at: http://irtfweb.ifa.hawaii.edu/Facility.

iSHELL is planned as a replacement for CSHELL, which had first light in 1993. CSHELL is a single-order echelle spectrograph and uses a single 256x256 InSb array[1,2]. CSHELL is one of only a few high-resolution 1-5 μm echelle spectrographs available to observers in the northern hemisphere. Capitalizing on technological developments in spectrograph gratings and infrared arrays iSHELL will provide greatly improved capabilities over CSHELL. The use of a Teledyne 2048x2048 Hawaii 2RG (H2RG) in the spectrograph combined with a cross-dispersed spectral format will increase the simultaneous wavelength coverage by about 30-60 times depending on wavelength. Also, by employing a silicon immersion grating to reduce the required collimated beam diameter, the resolving power will be doubled to R=75,000 while at the same time keeping the cryostat relatively compact. The addition of an infrared slit viewer for object acquisition and guiding will significantly improve observing efficiency.

Dan Jaffe's group at the University of Texas (UT) at Austin has invested much research and development effort into producing silicon immersion gratings for infrared spectrographs[3,4,5]. A high quality silicon immersion grating is used in the IGRINS spectrograph[6] (R=45,000, 1.4-2.5 μm simultaneously) that is currently in use on the 2.7 m telescope at McDonald Observatory, Texas. UT has built a similar high quality immersion grating for iSHELL.

The science drivers, design requirements and design of iSHELL were discussed in the previous paper[7]. In this paper we briefly review the design before discussing the construction, assembly and laboratory testing of iSHELL.

*rayner@ifa.hawaii.edu; phone 1 808 956-9846; http://irtfweb.ifa.hawaii.edu/

2. DESIGN OVERVIEW

Given the science case, the immersion grating size available to us, and the overall size of the instrument, we have chosen a resolving power of 70,000. Resolving power, R, is given by

$$R = \frac{2d}{\phi D} n \tan\delta \quad (1)$$

where d is the collimated beam diameter, D is the diameter of the telescope primary mirror (3 m for IRTF), ϕ is the slit width (radians), n is the refractive index of the immersion material, and δ is the blaze angle of the grating. To achieve good optical efficiency at the desired resolving power of R=70,000, the slit width is set to 0.375″ to match the best uncorrected seeing at IRTF with a selection of wider slits available. For good sampling the 0.375″ slit width is matched to three pixels. The practical requirements to keep the instrument small enough to mount at Cassegrain focus ($d \approx 25$ mm), and for good sub-pixel optical aberrations in the spectrograph (f/38 collimator), dictate the use of an R3 ($\tan\delta$ =3) silicon (n =3.4) immersion grating. R3 format is the standard format used by UT who have fabricated the immersion gratings for us. A white pupil spectrograph design is employed to keep the optical components and off-axis angles small. The immersion grating is placed at the first pupil and the cross-dispersing gratings at the second pupil. The immersion grating is illuminated in pseudo-Littrow (γ-angle =1.025 degree) for optimum grating efficiency and to reduce the potential for a 'picket fence' optical ghost[8]. The cross-dispersing gratings are replica plane-ruled reflectance gratings from Richardson Gratings used in first order.

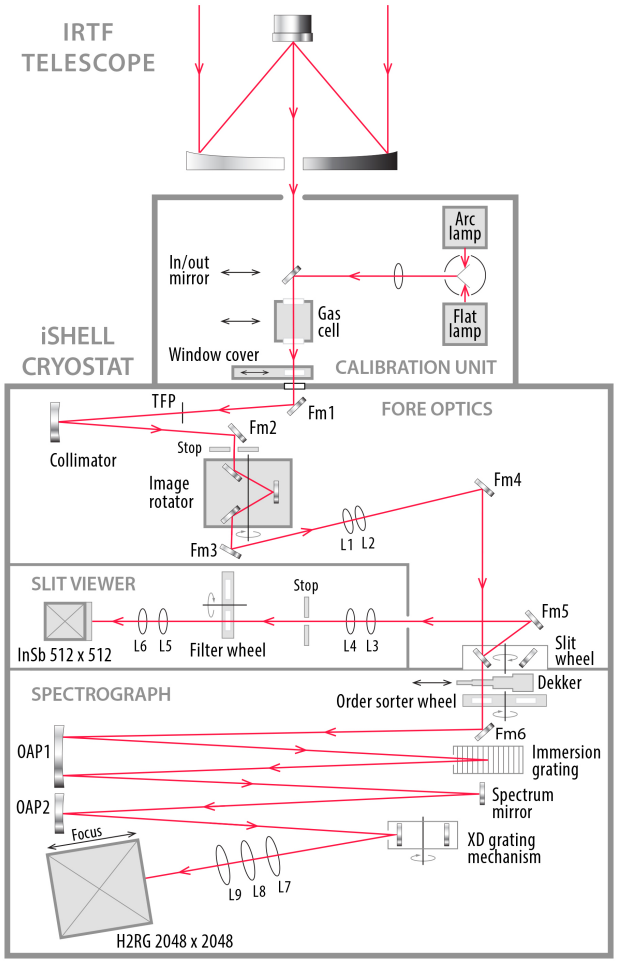


Figure 1. Schematic layout of iSHELL. The cryostat optics consists of three major components: foreoptics, slit viewer, and white-pupil spectrograph. A spectral calibration unit is located immediately outside the entrance window. There are eight cold mechnisms: image rotator, filter wheel, slit wheel, Dekker, order-sorter filter wheel, cross-disperser (XD) grating turret (rotate and tilt) and spectrograph focus stage**.** Fold mirrors (Fm) and the off-axis parabolas (OAPs) are also shown.

iSHELL requires fore-optics since it is necessary to place a cold stop before the slits as diffraction at the slits would otherwise blur the image of the telescope entrance pupil on a cold stop placed following the slits and result in higher backgrounds at thermal wavelengths. The cold stop is also the best place to baffle off-axis scattered light from the infrared-optimized (i.e. unbaffled) telescope. Also, since IRTF is an equatorial telescope and since iSHELL is too big to easily rotate, an internal K-mirror image rotator is used to change the position angle of the slit on the sky. To keep the K-mirror compact it is located immediately following the cold stop. The fore-optics is a simple collimator-camera arrangement that reimages the f/38 telescope focal plane (TFP) onto slit mirrors (mirrors with a transmissive slit) in a slit wheel. A second collimator-camera reimages the slit field onto the slit viewer array with a field-of-view (FOV) of 42″ diameter. A schematic of the optical layout is shown in Figure 1.

At resolving powers of *R*=*70*,000 there is effectively no sky and telescope background at 1-2.5 μm in between OH sky emission lines[7], and in a properly designed instrument sensitivity is limited by detector array dark current and read noise. To keep thermal background from the optical enclosure below the dark current (<0.1 e/s) requires an enclosure temperature of less than 78 K (see Figure 2). To achieve the required low dark currents the detector arrays must operate at about 35 K. In iSHELL liquid nitrogen cools the optical bench and enclosure, and a closed-cycle cooler cools a radiation shield and the arrays.

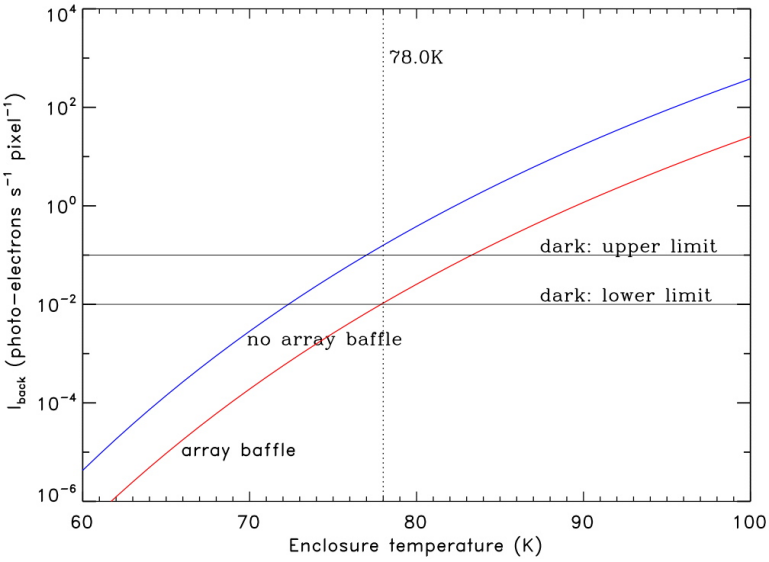


Figure 2. Background signal at a detector pixel is plotted as a function of enclosure temperature. The blue plot is for a half-angle field-of-view (FOV) of 90 degrees, and the red plot is for a half-angle FOV of 15 degrees (the practical limit for the iSHELL optical design) where a pixel's FOV is limited by a baffle at the same temperature as the detector array (37 K). Both plots assume a detector cut-off of 5.4 μm.

3. OPTICAL TOLERANCING AND FABRICATION

3.1 Optical Tolerancing and Specification

In the optics low-frequency spatial errors (~0.001-0.01 μm^{-1}) affect the core of the image profile and are analyzed with ZEMAX using the standard tolerancing parameters (e.g. thickness, radius, decentration, tilt, runout, surface irregularity, refractive index, inhomogeneity). Mid-frequency (~0.01-1 μm^{-1}) and high-frequency spatial errors (>1 μm^{-1} – roughness, the source of scattered light) affect the wider wings of the image profile and are analysed using a Power Spectrum Density function (PSD) method[9].

The science requirement is for a spectrograph resolving power $R \equiv \lambda/\delta\lambda \geq 70{,}000$, where δλ, the smallest resolvable wavelength, is taken as the Full Width at Half Maximum (FWHM); however, see Robertson (2013)[10]. In iSHELL the aberration-free diffraction-limited resolving power of *R*=80,000 is matched to three pixels. Using a Monte Carlo analysis (58 spectral configurations) and industry standard tolerances (see Table 1), 90% of the trials gave worst-case geometric 50% encircled energy dispersion widths better than 1.1 pixels (RMS wavefront error 0.11 μm at 1.65 μm). When added in quadrature with the diffraction-limited width of three pixels the FWHM is 3.2 pixels, equivalent to *R*=75,000.

The PSD represents the spatial frequency spectrum of the surface roughness measured in inverse-length units[9]. It can be calculated from surface profiles made by an optical or mechanical profiler. For typical optical quality surfaces, mid-frequency and high-frequency surface irregularity scales with the square root of the ratio of beam foot print to optical element diameter. The total wavefront error due to irregularity, σ_T, is given by

$$\sigma_T^2 = \sum_1^l \left[\sigma_l \left(\frac{FP_l}{D_l}\right)^{\frac{1}{2}} \frac{\lambda_t}{\lambda_u} (n-1)_l\right]^2 + \sum_1^m \left[2\sigma_m \left(\frac{FP_m}{D_m}\right)^{\frac{1}{2}} \frac{\lambda_t}{\lambda_u}\right]^2 \quad (2)$$

In the first term of the summation σ_l is the RMS surface error over the diameter D_l of the l^{th} lens surface (factor of *(n-1)* for surface refraction) measured at the wavelength it is tested λ_t and used at wavelength λ_u, *n* is the refractive index of

the lens medium, and $\boldsymbol{FP_l}$ is the diameter of the beam footprint at the l^{th} element. In the second term of the summation $\boldsymbol{\sigma_m}$ is the RMS surface error over the diameter $\boldsymbol{D_m}$ of the m^{th} mirror surface (factor of *2* for surface reflection) measured at the wavelength it is tested λ_t and used at wavelength λ_u, and $\boldsymbol{FP_m}$ is the diameter of the beam footprint at the m^{th} element.

Table 1. Standard fabrication and assembly tolerances

PARAMETER (ZEMAX CODE)	*VALUE*	*UNITS*	*NOTES*
Thickness (TTHI)	±0.10	mm	
Surface decentration (TSDX/Y)	±0.05	mm	
Element decentration (TEDX/Y)	±0.05	mm	
Element tilt (TETX/Y)	±0.05	degrees	
Lens runout (TIRX/Y)	±0.05	mm	
Lens thickness (TTHI)	±0.05	mm	
Radius (TRAD)	±0.1%	n/a	
Fold mirror (TIRR)	±0.2 P-V	Fr. @ 0.63 μm	Fringes measured at 0.63 μm over the clear aperture
OAP collimating mirrors	±0.125 P-V	Fr. @ 0.63 μm	Over 22 mm ϕ beam footprint
BaF_2 surface irregularity (TIRR)	±0.5 P-V	Fr. @ 0.63 μm	Clear aperture
ZnS surface irregularity (TIRR)	±0.5 P-V	Fr. @ 0.63 μm	Clear aperture
LiF surface irregularity (TIRR)	±1.0 P-V	Fr. @ 0.63 μm	Clear aperture
Refractive index, Δn (TIND)	±0.001	n/a	Bulk change of substrate
Inhomogeneity, Δn (TEZI)	$\pm 5 \times 10^{-6}$	n/a	Low order change of substrate

From the PSD analysis and using vendor estimates for surface irregularity and measurements for the immersion grating we estimate an RMS wavefront error $\sigma_T = 0.056$ waves at 1.65 μm. Using the Mahajan approximation the Strehl ratio, *S*, is given by

$$S \approx \exp -\left(2\pi\sigma_T\right)^2 \quad (3)$$

Therefore the Strehl ratio due to mid-frequency and high-frequency spatial errors is 0.88 at 1.65 μm. ZEMAX tolerancing of the image core (low-frequency spatial errors) gives an RMS wavefront error of 0.061 waves at 1.65 μm (with surface irregularity removed) and a Strehl ratio of 0.84. Therefore the total estimated Strehl ratio of the spectrograph is about 0.75 at 1.65 μm – close to the diffraction limit of 0.8. In general the delivered as-built parameters have proved to be better than the parameters specified in Table 1.

The spectrograph camera consists of an all-spherical surface BaF_2-ZnS-LiF triplet lens and was fabricated by ISP Optics (in-house production of LiF elements has since been discontinued). The lens diameters are 104 mm, 100 mm and 95 mm respectively. The combination of BaF_2 and LiF produces the best correction of chromatic aberration over the range 0.8-5.5 μm and the combination has been used regularly in IRTF instruments since 1993. Rather than adding more lenses, and increasing stray light, the small remaining chromatic focus effects are removed by using small movements of a focus stage for each of the spectrograph modes (range ± 1.0 mm). A problem with fluoride lenses, and LiF in particular, is that they are fragile and more difficult to machine and polish (hence the relaxed surface irregularity requirement of LiF in Table 1). Fortunately the effects of surface irregularity in the camera lens are significantly reduced since at its location away from a pupil, the beam footprints are small compared to the lens diameters (see Equation 1 and Figure 3).

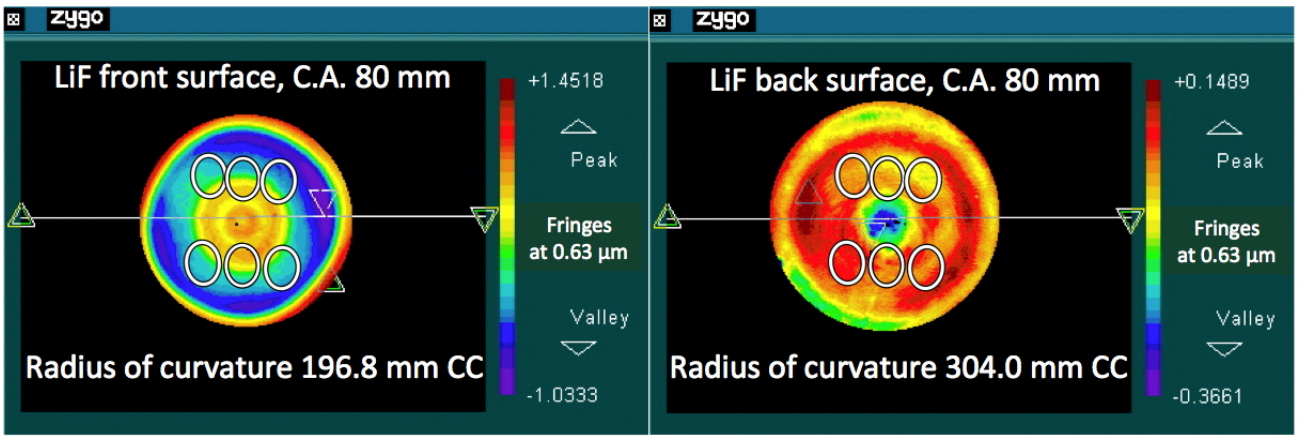


Figure 3. Zygo interferometer surface/wavefront maps for the 95 mm diameter LiF lens (clear aperture 80 mm) in the spectrograph camera. Also shown are beam footprints at the center and both ends of the free spectral range for top and bottom spectral orders in the K3 spectral mode (see Table 2).

Since the 95 mm diameter LiF lens is most susceptible to fracture on cooling, it was selected for finite element analysis (FEA). A similarly sized LiF lens in JWST/NIRcam was extensively modeled[11] and that analysis was used for reference. The three spectrograph camera lenses are mounted in an aluminum barrel. For optical precision each lens is held in place radially by a leaf spring pushing the lens against two fixed radial pads and held in place axially by three coiled springs pushing against three axial pads. The holding force is 2.5 N (10 g) and the lenses become radially centered on cooling. A similar arrangement is used to mount the smaller BaF_2-LiF doublet lenses in the foreoptics and slit viewer.

Analysis of the large LiF lens was done in two parts. A transient thermal FEA was followed by an internal stress FEA. The analysis included the effects of cooling by conduction and radiation, and contact resistance at the mounting points (400 W m^{-2} K^{-1}). We found that a cooling rate of less than 0.5 K min^{-1} was required to the keep the stress in the lens (1.25 Mpa) well below that recommended by the NIRcam analysis[11] (maximum resolved stress 2.0 Mpa). This is done by thermally isolating the aluminum lens barrel from the liquid nitrogen-cooled optical bench by fiber-glass washers. The assembly mounts to the bench by three pads and two pins for registration.

The two off-axis parabolic (OAP) mirrors are single-point diamond-turned (SPDT) from 6061-T6 aluminum so that alignment can be done warm and is not disturbed on cooling. SPDT aluminum has periodic structures (i.e. grooves) in the surface that can be a significant source of scatter. To reduce scatter the OAPs are fabricated from Rapid Solidification Process (RSP) aluminum. This is aluminum that is solidified by rapidly cooling from melt forming a very homogenous structure that machines without the 'pull outs' that cause the periodic structures. RSP Technology markets this material. Durham Precision Optics fabricated the OAPs and an integrated aluminum mount, which mounts to the bench by three pads and two pins. One company specializing in machining aluminum mirrors claims that the improved homogeneity is mostly lost once RSP material is cryo-cycled, as it must be for final figuring. However, we see no evidence for this in our delivered OAPs. OAP1 is 220 mm long, 80 mm wide and 20 mm thick; OAP 2 is 220 mm long, 46 mm wide and 20 mm thick (see Figure 1). An important part of the design was an FEA to minimize flexure in the OAPs and the OAP mount.

The slit mirrors are antireflection-coated CaF_2 substrates with a gold coating (optical depth > 10^3) and slit aperture lithographically applied to the frontside. A metal coating is also applied to the backside to absorb optical ghosts. The slit mirrors are inclined at 22.5 degrees to the incoming f/38 beam to reflect a 42″ diameter field into the slit viewer. Since the gold coating is less than one micron thick scattering due to the inclined edge of the slit is negligible. A very similar design was used successfully in SpeX[12]. The CaF_2 substrates are 30 mm diameter and 5 mm thick. Max Levy Autograph, Inc., fabricated the slit mirrors.

4. CONSTRUCTION

4.1 Cryostat

The cryostat consists of a warm box-shaped vacuum jacket, cold radiation shield, cold optical bench and light tight covers (photon shield). A liquid nitrogen can cools the optical bench and photon shield to about 77 K and the first stage of a 1050 CP closed-cycle cooler cools the radiation shield, which encloses the optical bench and photon shield, to about 130 K. The second stage of the cooler cools the spectrograph H2RG array to 37.00 K and the slit viewer Aladdin 2 array to 30.00 K. The immersion grating operates 80.00 K. LakeShore 335 temperature controllers provide temperature stabilities of ±0.005 K. This gives a wavelength stability of about 0.02 pixels for the immersion grating (a 2 K temperature change moves spectral lines eight pixels), which is ultimately limited by flexure in the instrument (see section 6.3).

Atlas Technologies fabricated the vacuum jacket. It is a four-sided TIG-welded Al 5056-T0 structure with two Al 6061-T6 covers. Al 5056-T0 is used for the main structure since it retains it strength and does not require heat-treating after welding. For optimum vacuum integrity the parts were milled from billets. All the service ports for wiring and cooling are machined into the central section. Removing one cover gives access to the fore-optics side while removing the other cover gives access to the spectrograph. The O-ring grooves are machined into the covers with a dovetail shape to prevent the O-rings from falling out during assembly and maintenance. The inside of the vacuum jacket is highly polished for low emissivity. No multi-layer thermal insulation is needed in iSHELL. The external dimensions of the vacuum jacket are 1.31 m x 0.70 m x 0.70 m. A telescope interface box is welded to the top plate of the vacuum jacket. This box contains the calibration unit (see Figure 1). The total weight of the vacuum jacket including the interface to the telescope is 265 kg.

The spectrograph and foreoptics are mounted on opposite sides of the optical bench, which is milled from a single ingot of aluminum 6061-T6. For positional precision final machining follows cryogenic cycling of the bench. In addition to pocketing and drilling access holes for optical and mechanism mounts, the bench contains covered channels for wiring to shield the detectors (5.4 μm cut-off) from potential thermal emission from the wiring. Two light-tight (except of the optical beam entry port) aluminum covers enclose the optical bench. The covers are highly polished on the outside for low emissivity and painted black (Aeroglaze Z306) on the inside to absorb scattered light. For cooling a 12 l capacity liquid nitrogen can, also made by Atlas Technologies, is bolted directly to the optical bench. The can is machined from an Al 6061-T0 billet with a TIG-welded cover added. Two stainless steel fill tubes connect the can to the fill port in the vacuum jacket. Each tube has a Swagelok bellows at the top and bottom for mechanical compliance on cooling. The fill tube assembly attaches to the liquid nitrogen can via an indium-wire sealed flange plate. Cardic Machine Products, Inc. fabricated the optical bench and photon shields. Four V-shaped titanium trusses attach the optical bench to the vacuum jacket. Titanium is used for stiffness, thermal isolation and ease of assembly. The weight of the optical bench including the photon shields and liquid nitrogen can is 102 kg and 202 kg with the mechanisms and optics added.

The radiation shield reduces the thermal load on the optical bench. It is made from six 3 mm thick Al 6061-T6 plates bolted together. It weighs 31 kg. The plates are highly polished for low emissivity. Several G-10 mounting tabs attach the shield to the vacuum jacket. The side covers corresponding to the side covers of the vacuum jacket contain no feed-throughs and are removable to give access to the foreoptics and spectrograph.

The total weight of the cryostat including all the optical components, mechanisms, and cryostat-mounted electronics boxes is about 520 Kg.

4.2 Mechanisms

iSHELL contains eight cold mechanisms (see Figure 1). The slit wheel, order sorter filter wheel and slit viewer filter wheel are detented Geneva mechanisms. When in position the wheels are immobile and decoupled from the drive. The wheel position is accurately defined by the detent and not by the drive train. The detent is lowered into position with a cam attached to the drive. The K-mirror image rotator requires continuous rotation and employs a worm gear. To remove backlash, the worm is radially preloaded against the worm gear with a wire-EDM fabricated parallel flexure stage. The spectrograph detector focus stage employs a planetary gear for gear reduction and a lead screw for translation (a few mm of focus are required), and the array mount is itself mounted on a parallel flexure stage, which only allows movement in

the focus direction. To remove backlash, a preloaded split nut is used for the lead screw. In the Dekker mechanism a mask with three sections defining the slit lengths is mounted on a stage attached with two parallel linkages that have flex pivots at both ends. A crankshaft and worm gear train drive the stage in a slightly arced motion. The arced motion is compensated for by the location of the individual slit masks.

The cross-disperser grating turret contains two mechanisms: a detented eight-position grating wheel and a tilt mechanism to tilt the entire wheel ±5 degrees about the optical axis parallel to the grating grooves through the center of the grating. A tilt mechanism is required to move spectral orders up and down on the array. The turret is rotated by a pre-loaded worm gear and is held accurately in position by an arm with a bearing at its end that rolls and drops into V-shaped detents. On the rotation axis a flexure-bearing mount compensates for contraction on cooling. In the tilt mechanism two large flex pivots are mounted along the optical axis on each side of the turret (see Figure 4) and a preloaded lead nut assembly pushes the turret around the tilt axis. Since the tilt mechanism is the most precise mechanism in the instrument (a tilt precision of 30 arcseconds is required for one pixel reproducibility) great care was taken to reduce backlash. The moving weight of the grating turret is 5 kg.

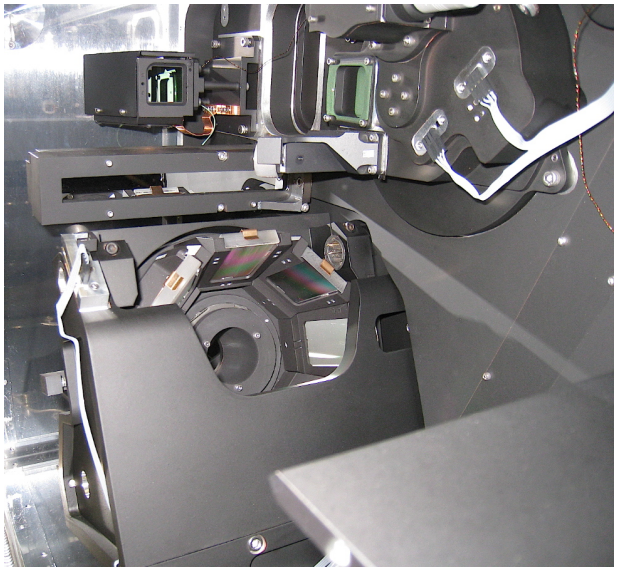


Figure 4. A view of the cross-disperser grating turret with the spectrum mirror and immersion grating above it.

The image rotator, cross-disperser grating turret and slit wheel are designed so the optical elements they carry are aligned both warm and cold. In order to compensate for thermal contraction between the stainless steel bearings and the aluminum wheels a standard approach is to have the bearing hub in the wheel fabricated with a larger diameter than the bearings at room temperature so that they become equal when cold. However, this approach does not allow for alignment at room temperature. For the alignment to be unchanged on cooling, an intermediate ring is added between the hub and each bearing. The rings have three protruding radial pads on leaf springs directly machined into them with a wire-EDM. At room temperature the hub is seated on the three pads, while at 77 K the three pads are compressed radially until the hub seats fully onto the ring.

All the cold mechanisms are driven with cryogenically qualified VSS-43 Phytron motors except the Dekker mechanism, which uses a smaller VSS-25 Phytron motor. All the metal gears in the mechanisms were coated with molybdenum disulphide (MoS_2) using a vacuum sputtering process. For the worm gear trains in the image rotator and cross disperser, the worms were fabricated from Vespel SP-3, which is a Polyimide plastic coated with MoS_2. All the ball bearings in the mechanisms were dry lubricated with MoS_2 using a spray and bake process. We used three bearing brands, Barden Bearings, W.M. Berg and Kaydon Bearings.

There are four warm mechanisms on top of the vacuum jacket in the vicinity of the entrance window: an ‘in/out’ fold mirror for selecting lamps from the calibration system, a widow cover, a gas cell in/out stage, and a ThAr lamp in/out stage. These are all driven by precision Micronix linear stages.

5. ASSEMBLY, TESTING AND OPTICAL ALIGNMENT

The assembly procedure of iSHELL is illustrated in Figure 5. This was done in the clean room in the IR Lab, Honolulu. The optical bench was lowered into the vacuum jacket using a gantry crane (Figure 6). Once the performance of the cryostat was qualified the mechanisms were installed and their function checked and fixed where necessary.

Preliminary warm testing of the mechanisms was done with warm-only Phytron motors. Following complete assembly it was still necessary to move the mechanisms when warm with the cryogenically qualified Phytron motors in order to complete sanity checks. However, the motors were not exercised for longer than about one minute in any one session and no problems with the Phytron motors have been encountered with continued warm and cold testing over one year in the lab. The optics were installed once the cold mechanisms were working properly.

To align the optics the beam was centered on each component in succession using an optical alignment telescope (OAT) mounted on the vacuum jacket at the window. The OAT was first auto-correlated on a mirror placed at the location of the first fold mirror immediately inside the window. This mirror was then replaced by an aluminum proxy for the actual fold mirror but with a fiducial cross on the optical axis. The mount was then centered and the proxy replaced with the actual fold mirror. A proxy was then placed in the following optical mount and the first mirror shimmed to center the beam. This procedure was repeated down the entire optical train. Analysis with ZEMAX indicated that a centering accuracy of one mm was required.

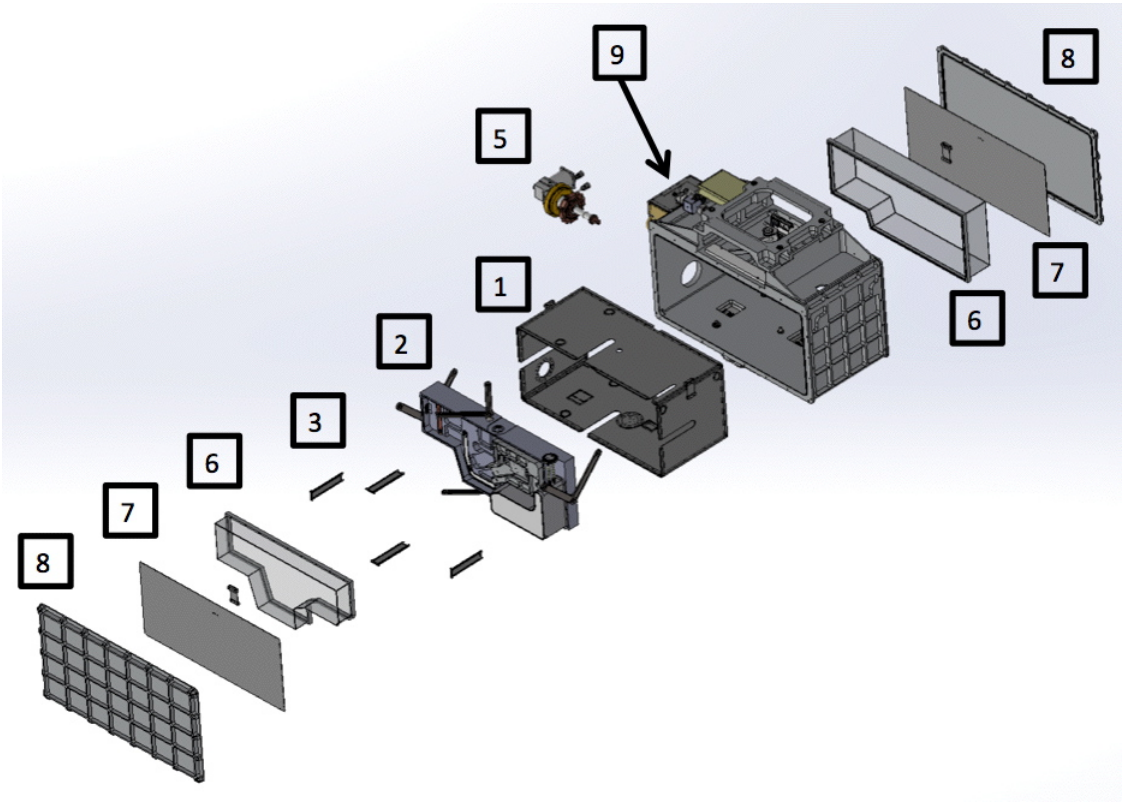


Figure 5. Stages in the assembly of iSHELL: (1) Install radiation shield into vacuum jacket. (2) Install optical bench with trusses attached. (3) Install truss covers into radiation shield. (4) Install wire harnesses (not shown). (5) Install cryo-cooler and thermal straps. (6) Install photon shields. (7) Install radiation shield covers. (8) Install cryostat covers. (9) Install array controllers. Mechanisms, optics and detector arrays are installed following satisfactory testing of the cryostat.

Initial alignment was done without the K-mirror image rotator in place and with a mirror in place of the immersion grating. Due to the 27-degrees of freedom (three mirrors each with three axes) it is difficult to align the mechanical axis of the K-mirror with the optical axis. Therefore the K-mirror was built as one machined assembly with tight specifications. Importantly, since it is located close to the cold stop (the pupil) in the foreoptics any misalignment does not move the reimaged pupil on the immersion grating in the spectrograph. Any misalignment at the slit (the reimaged telescope focal plane) when the position angle is changed is corrected by simply repointing the telescope. (Since IRTF is an equatorial telescope only one repointing is required for a given position angle.) The specification was for a misalignment on any rotation of less than 10% of the 42″ FOV of the slit viewer and this was met.

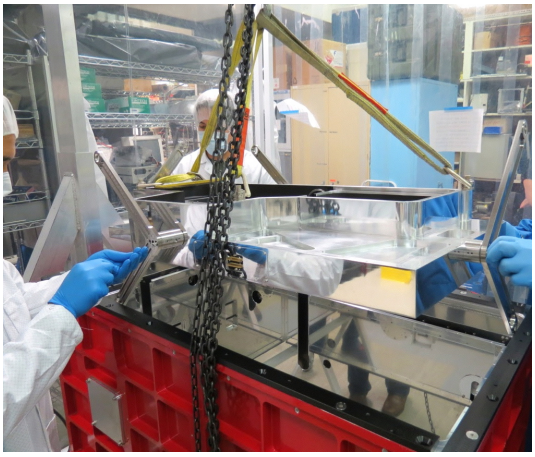


Figure 6. Installation of the optical bench into the vacuum jacket (stage 2 in Figure 5).

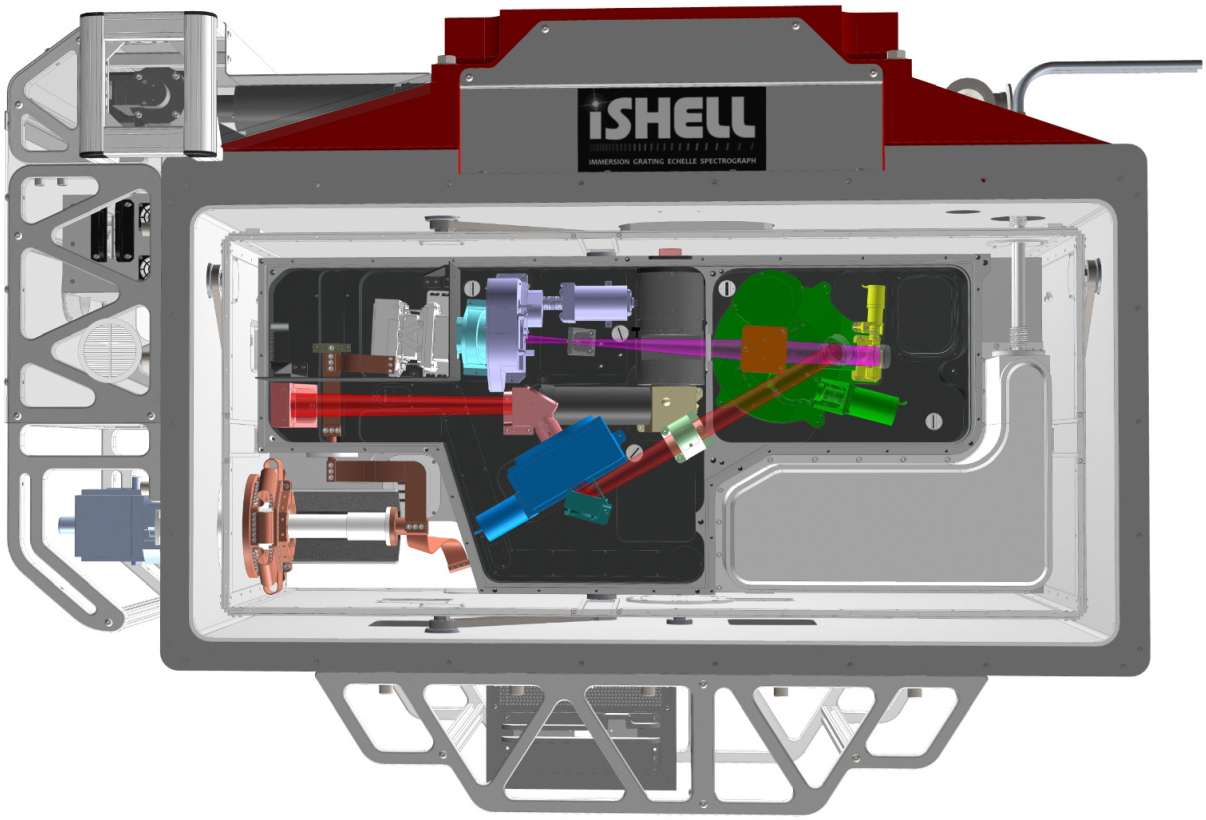


Figure 7. A view of the foreoptics side of iSHELL with the vacuum jacket cover, radiation shield cover and photon shield removed. Light enters from the top. The radiation shield encloses the optical bench. Four cold mechanisms are shown mounted to the optical bench: the image rotator (blue), slit wheel (green), Dekker (yellow), and slit viewer filter wheel (purple). The slit viewer array (grey) is at the top left. The first stage of the closed-cycle cooler (copper) attaches to the radiation shield and copper straps run from the second stage to the slit viewer array (top) and spectrograph array (bottom and behind). A liquid nitrogen can is bolted to the optical bench (lower right). A sub-plate above the slit viewer has been omitted for clarity. Mounted to the outside of the vacuum jacket is the spectrograph H2RG array controller (bottom) and the slit viewer Aladdin 2 array controller (top left). An integrating sphere is located immediately above the Aladdin controller. Aluminum frames protect the array controllers.

Following the initial optical alignment the proxy mirror is replaced with the silicon immersion grating. Since silicon is opaque in the visible the initial alignment of the immersion grating was done siting the reflection off the front face of the immersion grating. The front face is wedged by 0.8 degrees to avoid sending the undispersed ghost reflection towards the detector. The location of this ghost was modeled in ZEMAX and the tilt of the immersion grating was adjusted to position the ghost at the predicted location. Further small tilt adjustments were done following measurement of the blaze location on the array and correcting for vignetting of the long slit on the spectrum mirror during all-up cold tests.

Optical alignment of the instrument cold stop to the entrance pupil (the telescope secondary mirror) will be done by viewing the image of the secondary mirror on the cold stop using the pupil viewer optics in the slit viewer and by shimming the instrument mount.

Figures 7 and 8 show the layout of the instrument as rendered in ***SOLID****WORKS*.

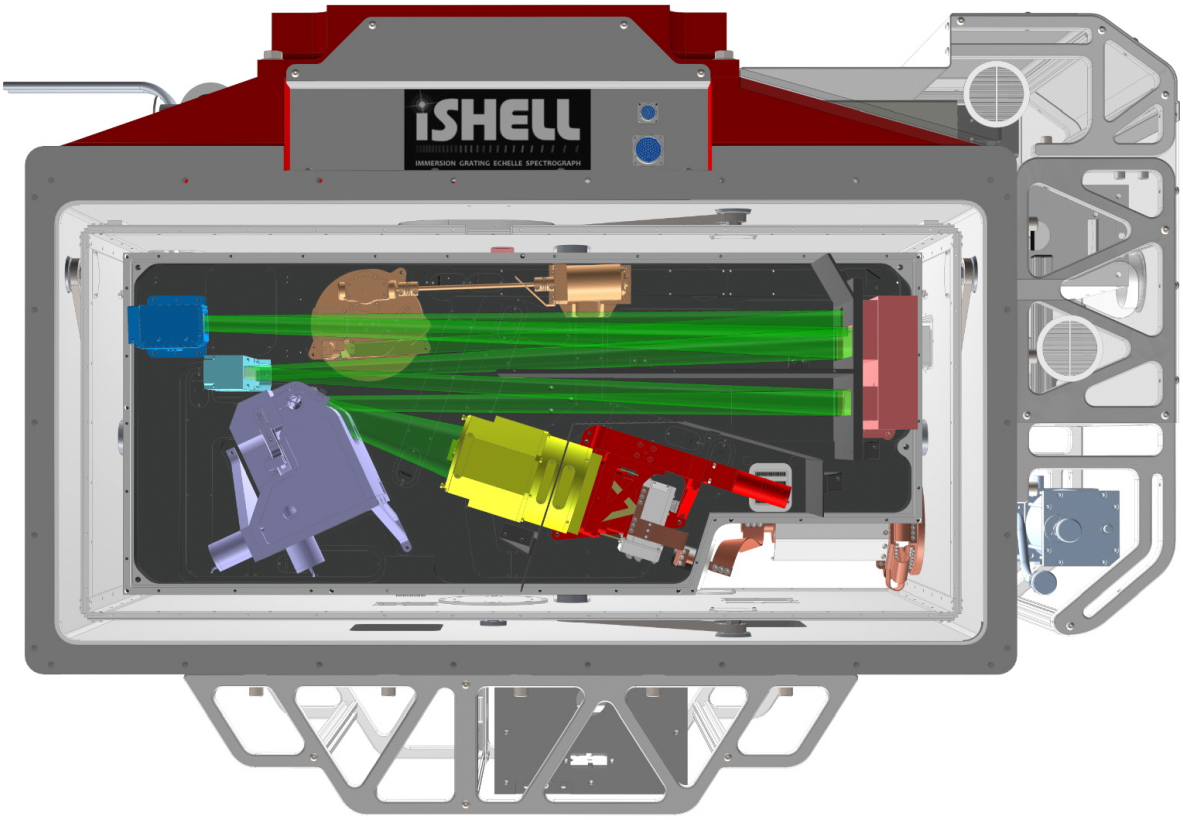


Figure 8. A view of the spectrograph side of iSHELL with the vacuum jacket cover, radiation shield cover and photon shield removed. The radiation shield encloses the optical bench. Four cold mechanisms are shown mounted to the optical bench: order sorter filter wheel (light brown), cross-disperser grating turret rotate and tilt (purple), and spectrograph array mount and focus stage (red). Optical components include the OAPs (pink), immersion grating (blue), spectrum mirror (light blue), and camera triplet lens (yellow). Light from the foreoptics enters the spectrograph through the slit and order sorter filter wheel (light brown). The spectrograph array (grey) is at the bottom right.

6. ALL-UP LAB TESTING AND PERFORMANCE

Lab testing of the fully assembled and integrated instrument started in November 2015 and as of this writing (May 2016) we plan to ship iSHELL to the IRTF for commissioning in July 2016. The all-up tests involved completing the optical alignment, extended cold testing of the mechanisms, flexure tests, optimizing software control and instrument characterization.

6.1 Cryostat

Following leak testing and evacuation with a turbo pump for typically two or three days the cryostat is pressure filled with liquid nitrogen. The detector arrays reach operating temperature after about nine hours and the immersion grating reaches its operating temperature of 80.00 K after about 15 hours. The body of the cross-disperser grating turret falls below 100 K after about 30 hours and requires about 200 l of liquid nitrogen. A plot of the measured spectrograph background signal measured at the H2RG array is shown in Figure 9. This is measured by blanking off the spectrograph at the slit and the measurement includes instrument background and detector dark current. It is the median across the whole H2RG array. The spectrograph reaches operating temperature after about 80 hours (background < 0.1 photo-electrons s^{-1}). In the lab the hold time of the liquid nitrogen can (12 l capacity) is about two days.

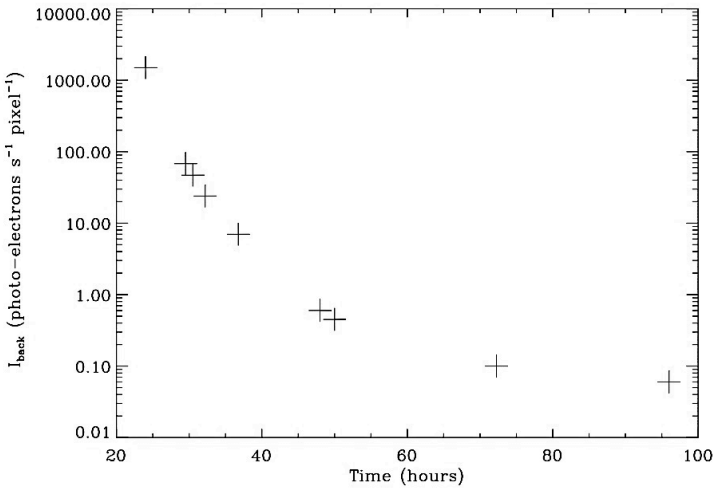


Figure 9. Measured spectrograph background signal, including dark current, during cooling. The signal bottoms out at about 0.06 e s^{-1} after about four days of cooling.

6.2 Optics

Final alignment of the optics required measuring the location of the peak of the blaze function on the array and, following warm up, re-machining the base of the immersion grating mount by the calculated amount to place the peak of the blaze in the central column of the array. The correction was then checked on cooling back down again. A similar procedure was required to align the long axis of the slits on the spectrum mirror by adjusting the base in the direction normal to the blaze correction. The silicon immersion grating and the grating in its mount are shown in Figure 10.

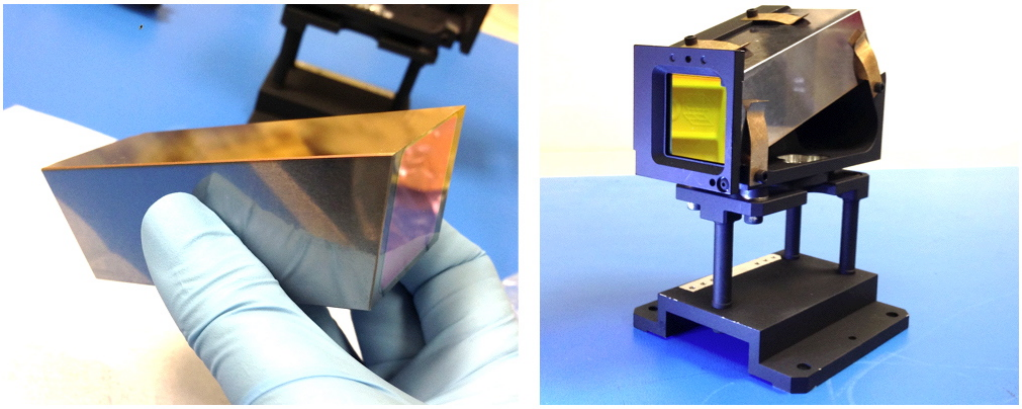


Figure 10. The silicon immersion grating (left) and the grating in its mount (right), shown without protecting cover. The base of the immersion grating mount required re-machining for final alignment. The grating is fabricated into the top surface of a silicon puck by a lithographic and etching process[3,4,5] (blaze angle 71.6 degrees and 12.5 grooves per mm). The front face of the immersion grating is 35 mm x 30 mm.

The performance of the spectrograph optics as measured by the FWHM of unresolved arc lines from a ThAr lamp is better than the specification of 3.3 pixels FWHM (R=72,000). Typical measurements are shown in Figure 10. One surprise is that useable transmission (>90 %) of the silicon immersion grating extends down to at least 1.1 μm. However, this is consistent with the low temperature absorption coefficients (α) recently measured by the Ligo project[13]. They find $\alpha > 0.005$ cm^{-1} for wavelengths shorter than 1.20 μm at 300 K but $\alpha > 0.005$ cm^{-1} for wavelengths shorter than 1.10 μm at about 80 K.

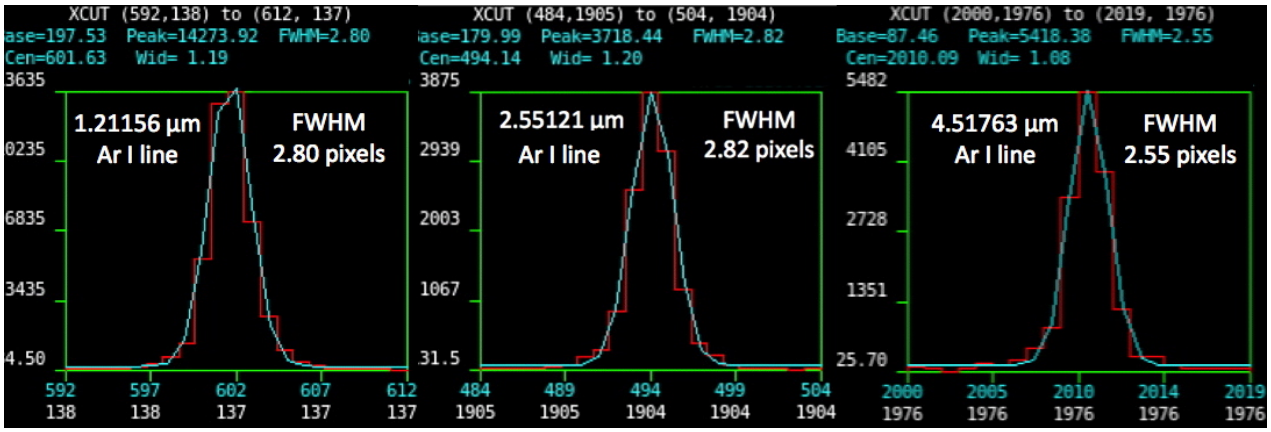


Figure 10. Typical Gaussian fits of the instrument profile on unresolved lines from a ThAr lamp (15 mA) through the 0.375″ slit (three pixels wide). The profiles are slightly better (narrower) than expected.

6.3 Instrument flexure

The IRTF is an equatorial telescope and iSHELL will used at Cassegrain focus. Therefore measuring the direction and magnitude of flexure in the instrument is very important. The most critical parameter is movement of spectral features in the dispersion direction affecting wavelength calibration. The specification is for any movement to be less than one tenth of the slit width (0.3 pixels) in one hour of observing (15 degrees of tilt in the RA direction) since wavelength calibration will be done typically once per hour. Shifts in the position of telluric absorption features in flat fields from the QTH lamp in the calibration system were measured as the instrument was tilted (see Figure 11). In the first tests we measured a movement of four pixels at +45 degrees and -45 degrees tilt in the declination direction and no measurable movement at +45 degrees and -45 degrees in the RA direction. At the same time no movement of the slit was observed in the slit viewer and so all the flexure was occurring in the spectrograph. The declination movement was improved to two pixels at +45 degrees and -45 degrees tilt by stiffening the base and adding a gusset to the OAP mount. The remaining flexure is probably coming from the cross-disperser grating turret since some movement is also seen in the cross-dispersion direction. More definitive tests will be done on the telescope but these preliminary tests indicate that the flexure specification is met.

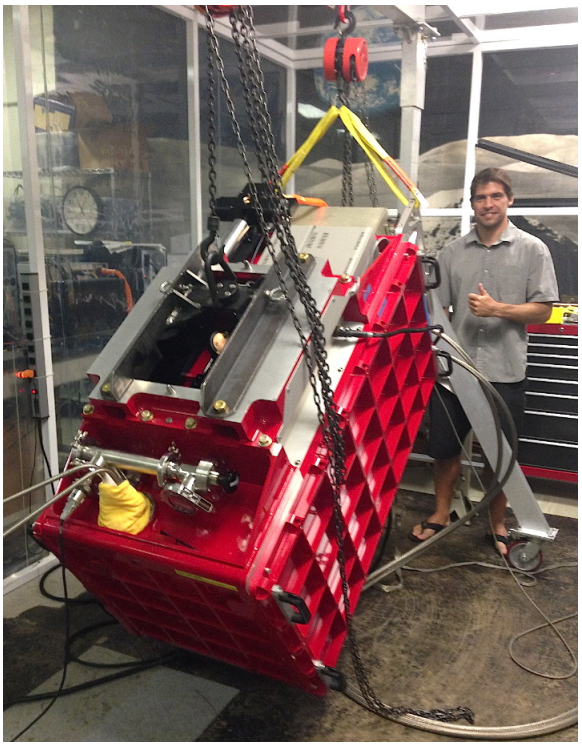


Figure 11. iSHELL suspended from a gantry crane and tilted 45 degrees in the equivalent of telescope declination. iSHELL weighs 520 Kg.

Flexure of the optical bench relative to the vacuum jacket and telescope will be measured by viewing movement of the telescope secondary mirror (the entrance pupil) relative to the cold stop in the slit viewer used as a pupil viewer. However, the titanium trusses holding the bench have been carefully

designed to minimize any movement. The primary purpose of the pupil viewer is to align the cold stop with the secondary mirror by shimming the instrument telescope mount. Any tilts causing movement at the telescope focal plane will be corrected by guiding.

6.4 Spectral formats

The spectral formats available with iSHELL are detailed in Table 2. In principle the XD tilt can be positioned to vary the wavelength limits at the choice of the observer but to simplify the initial data reduction tool there will be 18 fixed formats as indicated. Examples from lab testing are shown in Figure 12. Repositioning accuracy of the spectral orders is about ±2 pixels.

Table 2. List of cross-disperser gratings and spectral formats available in iSHELL. The wavelength ranges are preliminary and will be updated during instrument commissioning.

Mode	*Wavelength coverage (μm)*	*Order Sorter*	*XD tilt (degrees)*	*Slit length (arcsec)*	*XD (line/mm)*	*Blaze wavel. (μm)*	*Blaze angle (deg.)*	*Orders Covered*
J1	1.11-1.22	J_{OS}	53.8	5.0	1200	1.10	41.3	481-436
J2	1.20-1.30	J_{OS}	58.3	5.0	1200	1.10	41.3	442-405
J3	1.27-1.36	J_{OS}	61.8	5.0	1200	1.10	41.3	416-386
H1	1.48-1.67	H_{OS}	44.0	5.0	720	1.90	43.1	354-314
H2	1.55-1.74	H_{OS}	45.7	5.0	720	1.90	43.1	338-300
H3	1.64-1.82	H_{OS}	48.1	5.0	720	1.90	43.1	319-287
K1	1.94-2.23	K_{OS}	40.5	5.0	497	2.25	34.0	268-232
K2	2.09-2.38	K_{OS}	43.0	5.0	497	2.25	34.0	249-219
K3	2.26-2.55	K_{OS}	45.9	5.0	497	2.25	34.0	230-205
L1	2.74-3.02	L_{OS}	50.0	15.0	450	3.10	45.0	189-172
L2	2.96-3.24	L_{OS}	53.9	15.0	450	3.10	45.0	175-160
L3	3.20-3.43	L_{OS}	58.5	15.0	450	3.10	45.0	161-149
Lp1	3.27-3.65	L_{OS}	48.0	15.0	360	3.70	42.0	158-142
Lp2	3.59-3.93	L_{OS}	52.3	15.0	360	3.70	42.0	144-132
Lp3	3.83-4.14	L_{OS}	52.3	15.0	360	3.70	42.0	135-125
Lp4	3.83-4.14	L_{OS}	55.7	25.0	360	3.70	42.0	133-125
M1	4.55-5.27 s	M_{OS}	40.4	15.0	210	5.0	31.7	113-98
M2	4.55-5.27 l	M_{OS}	40.4	15.0	210	5.0	31.7	113-98

6.5 Calibration system

A spectral calibration unit is built onto the top of the vacuum jacket (see Figure 1). It consists of illumination optics, a 50 mm diameter integrating sphere from *Labsphere*, and flat field and arc lamps. The illumination optics, consisting of spherical mirror and BaF_2-LiF achromatic doublet lens, reimage the exit aperture of the integrating sphere onto the telescope focal plane inside the cryostat and also project a uniform pupil onto the immersion gratings where the telescope pupil is also located. Wavelength calibration is done with a ThAr lamp (P858A from Photron Ltd), and flat-field calibration with QTH (20 W 3200 K from Oriel) and blackbody (1100K IR element from Oriel) lamps. Elliptical concentrators feed flux from the flat-field lamps into the integrating sphere.

Originally the ThAr lamp was mounted to the integrating sphere but the arc lines proved to be too faint. This was fixed by moving the lamp directly over the entrance window. Due to ITAR restrictions no companies currently make ThAr lamps with pure Th cathodes. The Photron lamps use ThO_2, which leads to some spectral contamination and complicates arc line identification. Compared to the 1-2.5 μm range far fewer arc lines are available for wavelength calibration over the 3-5 μm range (see Figure 12) and so our plan is to make extensive use of telluric features for wavelength calibration.

Although iSHELL is not optimized for precision radial velocity science (precisions < 10 m s^{-1}) $^{13}CH_4$ and $^{15}NH_3$ gas cells for use at *H* and *K* have been provided by Peter Plavchan of Missouri State University. These can be moved directly into the telescope beam immediately above the cryostat widow.

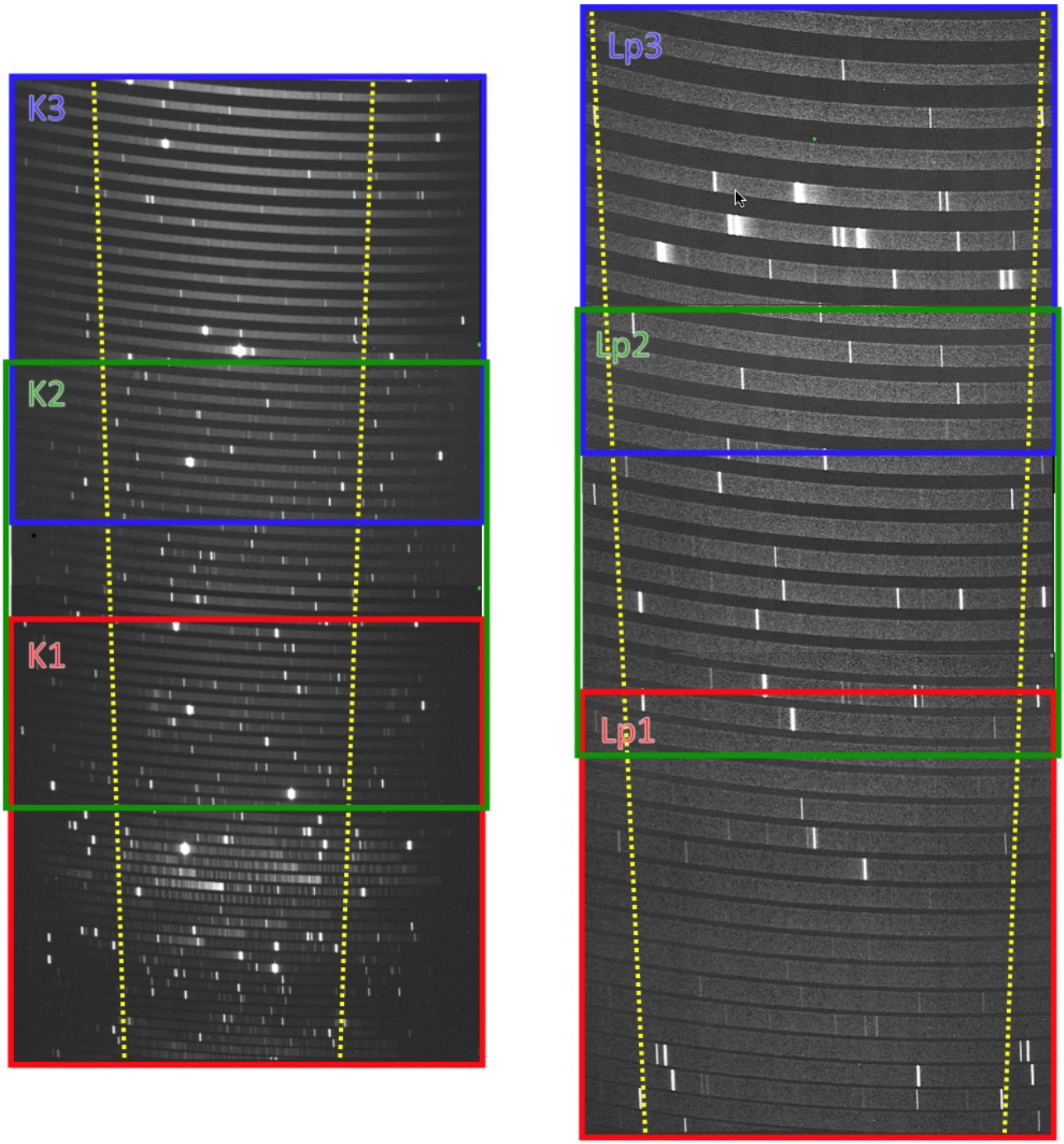


Figure 12. Example spectral formats (see Table 2). The images are 10 s mosaicked exposures of a ThAr arc lamp (15 mA) with the 0.375″ slit (R=75,000), lamp on minus lamp off. *Left K*-band mode showing three tilt positions of the cross-dispersing grating: K1 1.94-2.23 μm (red), K2 2.09-2.38 μm (green), K3 2.26-2.55 μm (blue). *Right L′*-band mode showing three tilt positions of the cross-dispersing grating: Lp1 3.27-3.65 μm (red), Lp2 3.59-3.93 μm (green), Lp3 3.83-4.14 μm (blue). In the *K*-band mode the slit length is 5″ and in the *L′*-band the slit length is 15″. The dashed yellow lines represent the approximate free spectral range.

6.6 Array and instrument control

Astronomical Research Camera (ARC) Generation 3 controllers are used for both arrays. Details of the design are discussed in the previous paper[7]. Identical controllers are already in use for the H2RG and Aladdin arrays in SpeX, which was successfully upgraded in 2014. One significant upgrade to the delivered ARC controllers was a new bias board with improved filtering to increase stability. The spectrograph H2RG array is wired for 32 outputs since we require integrations times as short as 0.4 s (300 KHz). One problem encountered during testing was that a couple of the 64-pixel wide channels would occasionally jump several tens of electrons relative to the other channels. This was remedied by optimizing Vbias-gate. Table 3 gives the measured performance of the H2RG array.

Table 3. Spectrograph H2RG array performance

Parameter	***Value***	***Note***
Gain	1.7 e/DN	Measured
Read noise NDRs= 1 NDRs=16	12 e RMS 5 e RMS	Measured at 3 μs/pixel
Dark current + instrument background	0.1 e/s	Measured at 0.312 V bias
Well depth	60,000 e	Measured at 0.312 V bias
Throughput at blaze 1.25 μm 1.65 μm 2.20 μm 3.60 μm 4.80 μm	0.08 0.16 0.18 0.17 0.16	Estimates only, including measured QE, optical witness samples, and grating efficiency curves

As with the other IRTF facility instruments, iSHELL is run via GUIs, one for the spectrograph and one for the infrared slit viewer/guider. Figure 13 shows the spectrograph GUI. Observers run the GUIs in Virtual Network Computing (VNC) desktop sharing sessions. Almost 80% IRTF observers now observe remotely.

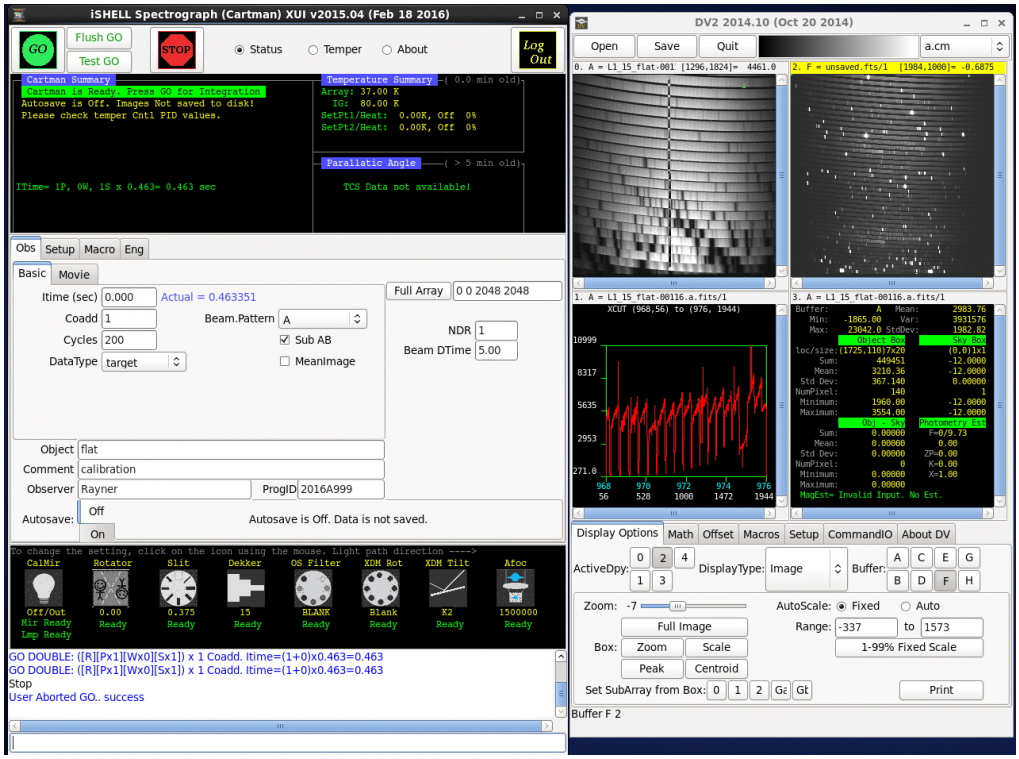


Figure 13. iSHELL's spectrograph GUI showing the instrument control GUI (left) and the Data Viewer display (right).

6.7 Data reduction

The data reduction package for iSHELL will be based on Spextool, the IDL-based package developed for SpeX[14] by Mike Cushing and Bill Vacca. They will also develop the iSHELL data reduction package. The major modifications required for iSHELL are spectral extraction for 18 spectral modes (see Table 2) compared to five for SpeX, a tilted slit (pseudo-Littrow orientation), more complex wavelength calibration using a combination of ThAr lines and telluric features, and the possible use of atmospheric modeling to remove telluric features in addition to A0V standard stars.

7. SUMMARY

Lab testing of the fully assembled and integrated instrument started in November 2015 and as of this writing (May 2016) we plan to ship iSHELL to the IRTF for commissioning in July 2016. General observing with iSHELL is scheduled to begin in October 2016. The all-up tests involved completing the optical alignment, extended cold testing of the mechanisms, flexure tests, optimizing software control and instrument characterization. Up-to-date information about iSHELL including current estimates of the sensitivity can be found in the iSHELL observing manual: http://irtfweb.ifa.hawaii.edu/~ishell/iSHELL_observing_manual.pdf.

ACKNOWLEDGEMENTS

We acknowledge the support of NSF award AST-0821866, NASA Contract number NNH14CK55B, and the University of Hawaii. We also thank former iSHELL mechanical engineers Tim Bond and Gary Muller for their contributions to the mechanical design, and Christ Ftaclas for teaching us about PSD analysis. Michael Mumma contributed significantly to the NSF proposal that we submitted for funding this instrument.

REFERENCES

[1] Tokunaga, A. T.; Toomey, D. W.; Carr, J.; Hall, D. N. B.; Epps, H. W.; "Design for a 1-5 micron cryogenic echelle spectrograph for the NASA IRTF", Proc. SPIE 1235, 131-143 (1990).
[2] Greene, Thomas P.; Tokunaga, Alan T.; Toomey, Douglas W.; Carr, Jonathan B.; "CSHELL: a high spectral resolution 1-5 μm cryogenic echelle spectrograph for IRTF", Proc. SPIE 1946, 313-324 (1993).
[3] Marsh, J. P.; Mar, D. J.; Jaffe, D. T.; "Production and evaluation of silicon immersion gratings for infrared astronomy", Applied Optics 46, 3400–3416 (2007).
[4] Wang, W; Gully-Santiago, M.; Deen, C.; Mar, D. J.; Jaffe, D. T.; "Manufacturing of silicon immersion gratings for infrared spectrometers", Proc. SPIE 7739, 77394L-1 - 77394L-9 (2010).
[5] Gully-Santiago, M.; Wang, W.; Deen, C.; Brooks, C.; Wilson, D.; Muller, R.; Jaffe, D.; " Near infrared metrology of high performance silicon immersion gratings", Proc. SPIE 8450, id. 84502S (2012).
[6] Chan Park, Daniel T. Jaffe, In-Soo Yuk, Moo-Young Chun, Soojong Pak, Kang-Min Kim, Michael Pavel, Hanshin Lee, Heeyoung Oh, Ueejeong Jeong, Chae Kyung Sim, Hye-In Lee, Huynk Anh Nguyen Le, Joseph Strubhar, Michael Gully-Santiago, Jae Sok Oh, Sang-Mok Cha, Bongkon Moon, Kwijong Park, Cynthia Brooks, Kyeongyeon Ko, Jeong-Yeol Han, Jakyoung Nah, Peter C. Hill, Sungho Lee, Stuart Barnes, Young Sam Yu, Kyle Kaplan, Gregory Mace, Hwihyun Kim, Jae-Joon Lee, Narae Hwang, Byeong-Gon Park; "Design and early performance of IGRINS (Immersion Grating Spectrometer)", Proc. SPIE 9147, id. 91471D (2014)
[7] John Rayner, Tim Bond, Morgan Bonnet, Dan Jaffe, Gary Muller, Alan Tokunaga; "iSHELL: a 1-5 micron cross-dispersed R=70,000 immersion grating spectrograph for IRTF", Proc. SPIE 8446, id. 84462C (2012)
[8] Robert G. Tull, Phillip J. McQueen, Christopher Sneden, David L. Lambert; "The High-Resolution Cross-Dispersed Echelle White-Pupil Spectrometer for the McDonald Observatory 2.7-m Telescope", PASP 107,251 (1995)
[9] John C. Stover; "Optical scattering: measurement and analysis", McGraw-Hill Inc. (1990)
[10] J. Gordon Robertson; "Quantifying resolving power in astronomical spectra", PASA 30, 48R (2013)
[11] E. Todd Kvamme, Dario Trevias, RaShelle Simonson, Larry Sokolsky; "A low stress cryogenic mount for space-borne lithium fluoride optics", Proc. SPIE 58770T-1 (2005)

[12] J.T. Rayner, D.W. Toomey, P.M. Onaka, A.J. Denault, W.E. Stahlberger, W.D. Vacca, M.C. Cushing and S. Wang; "SpeX: A Medium-resolution 0.8-5.5 Micron Spectrograph and Imager for the NASA Infrared Telescope Facility", PASP 115, 362-382 (2003)
[13] J. Degallaix, J. Komma, D. Forest, G. Hofmann, M. Granata, D. Heinert, C. Schwarz, R. Nawrodt, L. Pinard, C. Michel, R. Flaminio and G. Cagnoli; " Measurement of the optical absorption of bulk silicon at cryogenic temperature and the implication for the Einstein Telescope", Classical and Quantum Gravity 31, 18 (2014).
[14] Michael C. Cushing, William D. Vacca and John T. Rayner; "Spextool: A Spectral Extraction Package for SpeX, a 0.8-5.5 micron Cross-Dispersed Spectrograph", PASP 116, 362 (2004)